



This is a repository copy of *Thermal degradation profile mapping in stator coil insulation by impedance spectroscopy*.

White Rose Research Online URL for this paper:

<https://eprints.whiterose.ac.uk/226620/>

Version: Accepted Version

Article:

Stone, E.J.W. orcid.org/0009-0007-4795-9939, Panagiotou, P.A. orcid.org/0000-0001-5889-4412, Mühlthaler, J. et al. (3 more authors) (2025) Thermal degradation profile mapping in stator coil insulation by impedance spectroscopy. IEEE Transactions on Industry Applications. ISSN 0093-9994

<https://doi.org/10.1109/tia.2025.3544562>

© 2025 The Authors. Except as otherwise noted, this author-accepted version of a journal article published in IEEE Transactions on Industry Applications is made available via the University of Sheffield Research Publications and Copyright Policy under the terms of the Creative Commons Attribution 4.0 International License (CC-BY 4.0), which permits unrestricted use, distribution and reproduction in any medium, provided the original work is properly cited. To view a copy of this licence, visit <http://creativecommons.org/licenses/by/4.0/>

Reuse

This article is distributed under the terms of the Creative Commons Attribution (CC BY) licence. This licence allows you to distribute, remix, tweak, and build upon the work, even commercially, as long as you credit the authors for the original work. More information and the full terms of the licence here:

<https://creativecommons.org/licenses/>

Takedown

If you consider content in White Rose Research Online to be in breach of UK law, please notify us by emailing eprints@whiterose.ac.uk including the URL of the record and the reason for the withdrawal request.



eprints@whiterose.ac.uk
<https://eprints.whiterose.ac.uk/>

Thermal Degradation Profile Mapping in Stator Coil Insulation by Impedance Spectroscopy

Edward J. W. Stone, Panagiotis A. Panagiotou, *Member, IEEE*, Johannes Mühlthaler, *Student Member, IEEE*, Andreas Reeh, Alexis Lambourne, and Geraint W. Jewell

Abstract—Impedance spectroscopy is one of the continuously developing tools deployed for the inspection and evaluation of the health condition of electrical machines and machine components. Being a practical implementation and expansion of the Broadband Dielectric Spectroscopy (BDS) and the Electrochemical Impedance Spectroscopy (EIS), it allows the characterization of components by their amplitude and phase responses over frequency and the system's resonances. To this direction, this paper presents a study on the effect of thermal degradation on the insulation system of concentrated stator coils from the stator winding of a 2 MW permanent magnet synchronous generator purposed for aerospace applications. The thermal aging pattern and degradation mechanisms of the coil insulation are discussed through experimental results by *ex-situ* impedance spectroscopy.

Index Terms—impedance spectroscopy, insulation degradation, stator coil inspection

I. INTRODUCTION

AMONGST electrical machine components, electrical insulation systems are the most critical ones in terms of safety, endurance, and reliability [1]-[3]. Therefore, electrical insulation systems have traditionally been attracting significant research interest in terms of design, material characterisation and behaviour, degradation mechanisms, as well as health condition assessment and inspection [4]-[7]. This interest has evolved in tandem with technological developments in insulating materials, application-specific requirements and operational conditions, and testing hardware for health inspection and diagnostic strategies.

Impedance spectroscopy is a testing and inspection method broadly deployed for the health condition assessment and identification of the failure mechanisms in electrical machine components, such as insulation systems and materials [8]-[11]. The frequency sweep allows a full characterisation of the specimen by evaluation of the total complex impedance as well as resonance frequency and amplitude. As this is a transfer function in complex form, this analysis is facilitated by the Bode plots for the frequency responses and by the Nyquist plots

for characterisation of the system stability via the locus of the real and imaginary components [12]-[14].

The non-destructive nature of this technique is the primary reason for spectroscopy gaining significant attention from the research community for health monitoring and condition assessment in electrical machines. As such, several published works to this direction have investigated its potential in studies for several aspects, from the testing and characterisation of insulation specimen, stator windings and cores, or phase-to-ground measurements, to investigations examining stress factors and insulation degradation [15]-[20]. Compelling results have also been presented for the detection of abnormalities such as the existence of faults at incipient levels and inherent manufacturing defects [8], [14], [21]-[23].

Degradation and failure mechanisms are aspects of particular interest for electrical machine insulation systems, as they are critical to understand and predict, so that health condition assessment can reliably conclude on operational and life-limiting thresholds over the electrical machine lifespan. Electrical faults caused by insulation damage will always lead to short circuits. Depending on its location, a short-circuit can either be an inter-turn short circuit between the turns of a coil, a phase-to-phase short or a phase-to-ground short [1], [10], [24]. All electrical stresses imposed by the fault will result in thermal overload and cause fault propagation with risk of damaging the inverter driving the machine, or the cooling system, etc. To prevent such problems, monitoring and inspection of insulation systems is an essential mitigation strategy for the reliable identification of the insulation state over the machine lifecycle.

This paper examines the effect of thermal degradation on the coil insulation from the stator winding of a 2 MW permanent magnet generator deployed in the flight demonstrator of a hybrid aircraft [14], [25]-[30]. A group of coils from the generator winding have been aged thermally up to 1400 hours at the rated operational temperature for this insulation class; using impedance spectroscopy after every thermal cycle, the

This work was supported by the Aerospace Technology Institute (ATI UK) and Innovate UK via the project REINSTATE (Project 51689).

Corresponding Author: Panagiotis A. Panagiotou

E. J. W. Stone is with the School of Electrical and Electronic Engineering, University of Sheffield, S1 3JD, Sheffield, U.K., (e-mail: e.j.stone@sheffield.ac.uk).

P. A. Panagiotou is with the School of Electrical and Electronic Engineering, University of Sheffield, S1 3JD, Sheffield, U.K. (e-mail: p.panagiotou@sheffield.ac.uk).

J. Mühlthaler is with Rolls-Royce Electrical Ltd. & Co., 80335 Munich, Germany (e-mail: johannes.muehlthaler@rolls-royce-electrical.com).

A. Reeh is with Rolls-Royce Electrical Ltd. & Co., 80335 Munich, Germany (e-mail: andreas.reeh@rolls-royce-electrical.com).

A. Lambourne is with Rolls-Royce Central Services, Rolls-Royce Plc UK, DE24 9HY, Derby, U.K. (e-mail: Al.Lambourne@rolls-royce.com).

G. W. Jewell is the School of Electrical and Electronic Engineering, University of Sheffield, S1 3JD, Sheffield, U.K. (e-mail: g.jewell@sheffield.ac.uk).

coils were measured and characterised ex-situ. Using the Bode and Nyquist plots, the changes in the pattern of the frequency responses were studied to investigate the thermal degradation effect on the insulation. This analysis facilitates a holistic characterisation of the coil insulation system behaviour under the effect of thermal degradation to conclude on the aging profile of the coil insulation in terms of solely thermal stresses. The impedance profiles extracted from measurements are also investigated by simulations using a Finite Element Analysis (FEA) model that confirms the measurement observations.

II. INSULATION DEGRADATION & IMPEDANCE SPECTROSCOPY

A. Insulation Stresses and Degradation

The insulation in the stator windings of electrical machines is subject to several stresses. The primary ones are the TEAM stresses, as an abbreviation for thermal, electrical, ambient, and mechanical stresses. These always occur in combination with each other and at different intensity, which makes the evolution of the aging profile unstable and unpredictable [1], [6], [31]. They also coexist in tandem with Partial Discharges (PD), and high frequency stresses, each of which may come with different intensity and aftermath depending on the application and operational conditions [32]-[34]. The degradation of insulation in an electrical machine is mainly caused by thermomechanical and electrical loadings and create local hot-spots due to inherent manufacturing defects. Thereby, the first minor damages and defects of insulation may be introduced at the manufacture stage of the coils by deformation during pressing and bending. Besides, asynchronous loads and variability in the thermal stresses as well as adverse environmental conditions intensify the discussed stresses and accelerate the insulation degradation mechanisms [35]-[37].

B. Impedance Spectroscopy in Electrical Machines

From early studies, spectroscopy has been investigated widely for purposes of testing, ex-situ inspection and condition assessment as well as partially in-situ with both low and high voltage strategies. As a measurement, it evolved through the early practice of dielectric spectroscopy, which allowed the characterisation of material specimens, electrical components such as stator winding insulation samples, copper bars and insulation systems, etc. by the response of the dielectric permittivity over the frequency spectrum. The acquired measurements revealed the condition of the tested component by tracking the changes and the evolution of the intrinsic material properties in the complex permittivity. This also allowed the examination of the dissipation factor and power factor as means for validation of results [38]-[42]. Over the last two decades with the developments in this area of research as mentioned in Section I, impedance spectroscopy gained more and more ground [8]-[14]. The main reason is that it enables the analysis of the component or system under test, while facilitating an equivalent circuit analysis through the frequency domain representation of the global impedance. This approach allows to identify the order of the system in electrical circuit terms and examine its stability by means of a transfer function

of the equivalent circuit. This is provided by the impedance Bode plots, which render information regarding the amplitude and phase response and the system's electrical resonances.

Another advantage of this measurement is that it provides the ability to examine the impedance function with the Nyquist plots, representing the locus of the impedance real and imaginary components over frequency [8], [10], [12]-[14]. Lately, impedance spectroscopy has attracted increased interest from the research community as well as the industry as a key enabler by means of a non-destructive measurement for the detection of manufacturing deficiencies, material anomalies, faults at incipient levels, thermal, mechanical, and electrical stresses studies, as well as for trending the impact of combined stresses, including environmental. Characteristic research works in the literature with adequate reviews and detailed information on dielectric and impedance spectroscopy with compelling case studies can be found in [8]-[23] and [43]-[49].

III. EXPERIMENTAL SET-UP & COIL MODEL

A. Test Hardware

Each coil examined in this study is a structure as shown in Fig. 1a. The coil insulation system consists of several layers, shown in Fig. 1b. Each coil consists of compressed bundles of enamelled wire, labelled as Nr. 1 in Fig. 1b. Each wire strand is PAI-coated and bonded with epoxy-based resin (Nr. 2) for adhesiveness by vacuum pressure impregnation (VPI). The turn insulation is seen between each copper bundle (Nr. 3). The groups of conductors are covered by a double layer of groundwall insulation (Nr. 4 & Nr. 5), visible between the two bundle columns, and covered with conductive tape overcoat for enhanced electrical and thermal endurance (Nr. 6). The coil insulation layers of Fig. 1b are presented through Table I.

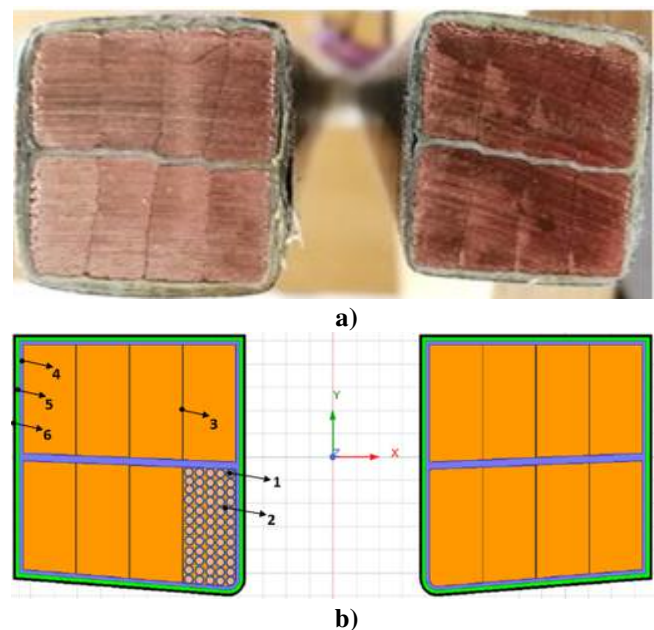


Fig. 1. Structure of the stator coils examined under thermal aging: a) Cross-section of a cut coil, b) schematic of coil sides in FEA model and insulation system layers: 1. Enamel wire

(PAI-coated), 2. VPI resin, 3. Turn insulation, 4. & 5. groundwall insulation, 6. Protective PET tape.

TABLE I
INSULATION SYSTEM LAYERS

Insulation Component	Insulation Type	Thickness
1. Copper Conductors	Litz wire, PAI-coated	–
2. Impregnation varnish	VPI resin	–
3. Turn insulation	Polyimide film	0.05 mm
4. & 5. Groundwall insulation	Glassfabric mica film	0.32 mm
6. Protective tape overcoat	PET/glasscloth	0.2 mm

These coils are from the stator winding of a 2 MW PMSG in the flight demonstrator rig of a hybrid aircraft [14], [25]-[30]. The PMSG has a concentrated stator winding that consists of the individual coil assemblies shown in Fig. 2, labelled as “Coil 1–Coil 4” (C1-C4). The stator coils were aged thermally using the oven system shown in Fig. 3a. The impedance spectroscopy measurements prior to and after each thermal aging cycle have been performed using the instrumentation depicted in Fig. 3b, which is a high resolution impedance spectroscopy analyzer (WK-1J6500B) allowing testing at frequencies up to 120 MHz at low voltage. The impedance analyzer was used after each thermal aging cycle to collect the data pertaining to the coil spectroscopy. Initially, the data were used for the examination of the impedance response by the Bode plots enabling the characterization of the coils and the insulation system. Then, the effect of thermal aging by racking the aging profiles of the coil insulation were examined through the changes in the frequency response by means of the Bode and Nyquist plots.



Fig. 2. Stator coils used as test hardware (C1 – C4).

The rated operational temperature for this insulation system

is 180°C (class H insulation), so the thermal degradation process consisted of exposure at 200°C for 100 hours per thermal cycle. After every 100-hour cycle of aging, the coils were taken out of the oven and left to cool at room temperature for 48 hours before being measured with the impedance analyzer. This process was repeated until 1400 hours of aging were achieved. Although this process ages the coil insulation by exposure at high temperature, it is not considered accelerated aging as the temperature is only slightly above the rated operating one for this class of insulation, so within the tolerance of operating conditions. The rationale for this choice of aging is to gradually acquire a degradation profile by emulating the operational thermal stresses naturally at this temperature, rather than accelerating them.



Fig. 3. Thermal degradation setup and measuring equipment: a) oven used to thermally age the coils and extractor, b) impedance analyzer WK-1J6500B.

IV. RESULTS

A. Experimental Measurements

The amplitude response and the phase response over the frequency spectrum for C1 are depicted in Fig. 4a and Fig. 4b, respectively. As described in [14], these Bode plots enable the characterisation of the coils showing the low frequency resonance in the frequency area of ≈ 2 MHz being a parallel equivalent, and the high frequency resonance which is a series equivalent in the spectrum area of ≈ 20 MHz. Due to space limitation, graphical results from only one coil are shown as the analysis and thermal degradation mechanisms are the same for all four coils. However, the tables present the experimental results from all coils in the set. As seen in Fig. 4, there is a shift towards higher frequencies for both resonances followed by an increase in the coil impedance while the aging progresses every 100 hours. The values of these changes in impedance are presented in Table II for all coils examined in this study. Through this table, the amplitude of the impedance rises from 2.1 k Ω to 3.61 k Ω for C1, from 2.1 k Ω to 3.5 k Ω for C2, from 2.24 k Ω to 3.54 k Ω in C3, and from 2.48 k Ω to 4.25 k Ω in C4. Expectedly, the angle of the impedance during the transition from these two resonance points will be zero due to match between inductive and capacitive components; this means that the global impedance of the coil will virtually have only a real part. Similar changes are seen at the high frequency resonance, where the frequency shift is followed by a decrease in the coil impedance amplitude with the aging progression. These values are summarised for all coils in Table III. For this frequency, the

impedance amplitude drops from 4.3 Ω to 3.17 Ω for C1, from 4.09 Ω to 3.45 Ω in C2, from 3.55 Ω to 3.32 Ω in C3, and from 4.05 Ω to 3.31 Ω in C4. By the characterisation of the coil assemblies through both tables and Fig. 4, it is seen how both the high and low impedance resonances are drawn towards higher values in the spectrum with the progression of thermal aging; further, in terms of impedance amplitude, the exposure of the coils at temperature results in amplitude increase at the low and a decrease at the high resonance, respectively.

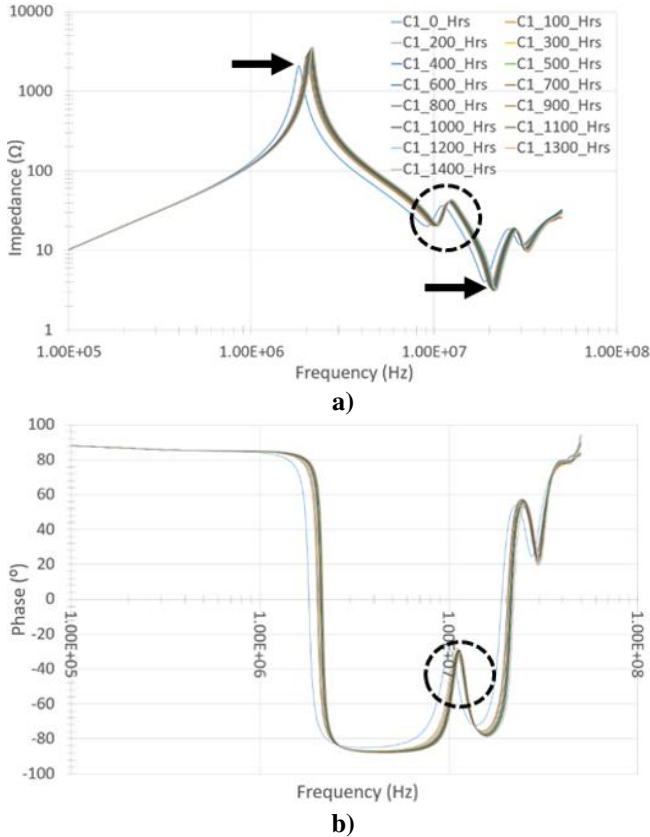


Fig. 4. Impedance spectroscopy – Amplitude & phase response of coil C1 from 0 to 1400 hours of aging: a) amplitude response, and b) phase response.

The peaks corresponding to the low resonance of the impedance response are shown in Fig. 5 for all hours of thermal aging, with this figure providing a close view of that frequency area only. Starting from the unaged coil which is the very first plot on the left hand-side of the graph (blue line), this peak shifts towards the right for every interval of aging. Although the first change in the impedance is quite tangible, the thermal aging profile after this first change at 100 hours evolves relatively slow. The trend line of these peaks at the first resonance is shown in Fig. 6 for all the coils with respect to frequency for all the hours of thermal degradation. This shows a linear increase in the impedance amplitude at this point, which is also seen from Table II. Only one of the coils (C4) performs as an outlier in terms of amplitude, which can be attributed to minor manufacturing tolerances [14]. However, the trendline remains consistent as a degradation profile over the span of the

coil's useful life as all the other coils in the set [50].

TABLE II
IMPEDANCE AMPLITUDE OF COILS C1, C2, C3, C4 FOR
THERMAL AGING FROM 0–1400 HOURS
(LOW RESONANCE FREQUENCY)

Hours	Coil Impedance Amplitude (k Ω)			
	C1	C2	C3	C4
0	2.1	2.1	2.24	2.48
100	2.82	2.7	2.76	3.1
200	2.84	2.72	2.83	3.22
300	2.96	2.84	2.91	3.36
400	3.05	2.95	2.99	3.49
500	3.17	3.01	3.06	3.65
600	3.19	3.05	3.12	3.68
700	3.28	3.19	3.22	3.83
800	3.29	3.28	3.32	3.99
900	3.33	3.33	3.34	4.01
1000	3.47	3.41	3.41	4.09
1100	3.44	3.41	3.44	4.11
1200	3.55	3.49	3.47	4.19
1300	3.54	3.48	3.51	4.11
1400	3.61	3.5	3.54	4.25

TABLE III
IMPEDANCE AMPLITUDE OF COILS C1, C2, C3, C4 FOR
THERMAL AGING FROM 0–1400 HOURS
(HIGH RESONANCE FREQUENCY)

Hours	Coil Impedance Amplitude (Ω)			
	C1	C2	C3	C4
0	4.03	4.09	3.55	4.05
100	3.55	4.05	3.43	3.95
200	3.61	4.07	3.48	3.92
300	3.50	3.99	3.41	3.86
400	3.39	3.86	3.30	3.80
500	3.31	3.83	3.27	3.53
600	3.28	3.76	3.37	3.49
700	3.30	3.69	3.26	3.39
800	3.33	3.59	3.26	3.81
900	3.14	3.55	3.25	3.33
1000	3.15	3.52	3.22	3.30
1100	3.13	3.48	3.24	3.25
1200	3.14	3.48	3.25	3.23
1300	3.23	3.49	3.28	3.28
1400	3.17	3.45	3.32	3.31

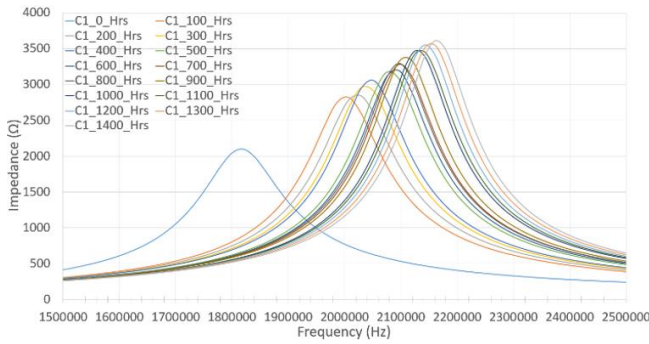


Fig. 5. Change in the impedance amplitude and resonance frequency of C1 from 0–1400 hours of thermal ageing.

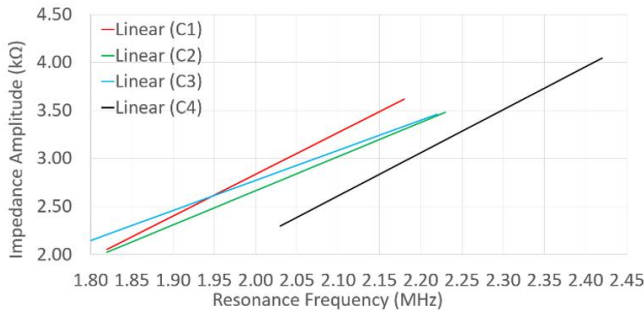


Fig. 6. Comparative plot of the thermal ageing profiles for the impedance of all coils (C1: red, C2: green, C3: blue, C4: black) versus the changes in resonance frequency (0 – 1400 hours).

A particular point of interest is the transient peak in the impedance response circled with dash line in Fig. 4. At this point, the complex impedance has transitions between a capacitive and inductive equivalent before moving towards the high end of the spectrum to a predominantly capacitive effect, with this transient peak change corresponding to a very narrow band of the spectrum. The values of this peak are shown in Table IV for the examined coils set with respect to the hours of degradation up to 1400 hours of thermal cycles. The values of the real and imaginary components of the total complex impedance are presented in Tables IV and V, respectively. These correspond to the transient peak circled with dash line in both plots of Fig. 4. Through Table IV, it is seen that although the real component persistently increases as it was the case in Table I, it does not change in this case as drastically as in the case of the first resonance. Further, it can be seen through Table V that the reactive part of the total complex impedance of the coil is also increasing. However, the angle between the real and imaginary components shows to slightly elevate by only a very minor change, which is very insignificant and can be practically considered to remain the same. This indicates a variability with increasing trend in the amplitudes of the total resistive and reactive components of the total complex coil impedance with respect to the hours of thermal aging, while the phase lag between them remains constant. As such, a representation of the locus of these two components such as the Nyquist plot can render very useful diagnostic information during inspection by means of impedance spectroscopy measurements.

TABLE IV
RESISTIVE PART OF IMPEDANCE FOR THE COILS C1, C2, C3, C4
FOR THERMAL AGING FROM 0–1400 HOURS
(TRANSIENT PEAK)

Hours	Coil Impedance Real Part (Ω)			
	C1	C2	C3	C4
0	25.99	27.57	28.14	27.91
100	26.88	30.58	30.93	29.51
200	26.45	30.51	32.22	30.60
300	26.37	30.05	33.31	31.94
400	27.07	29.36	32.62	31.18
500	27.42	30.93	33.95	32.94
600	27.68	31.25	32.20	33.36
700	28.14	32.36	33.26	31.65
800	27.97	31.83	34.44	31.64
900	26.90	32.29	33.29	31.88
1000	26.96	31.84	32.82	32.83
1100	27.08	32.57	33.90	30.95
1200	28.03	33.19	34.88	31.60
1300	28.72	33.30	35.16	31.66
1400	27.44	32.64	34.77	30.22

TABLE V
REACTIVE PART OF IMPEDANCE FOR C1, C2, C3, C4 FOR
THERMAL AGING FROM 0–1400 HOURS
(TRANSIENT PEAK)

Hours	Coil Impedance Reactance (Ω)			
	C1	C2	C3	C4
0	25.71	21.97	24.94	28.03
100	29.93	28.11	28.69	31.77
200	29.73	27.68	27.51	32.59
300	30.29	27.61	28.42	33.48
400	29.91	31.13	29.97	35.98
500	31.15	31.12	28.65	33.40
600	30.97	30.94	32.33	33.87
700	31.06	30.46	30.98	35.48
800	31.30	30.70	30.44	36.96
900	32.28	30.60	31.68	36.49
1000	32.92	31.89	32.41	35.49
1100	32.79	31.75	32.45	36.95
1200	32.49	30.96	31.53	36.16
1300	33.20	31.69	31.03	36.32
1400	34.06	32.53	33.13	38.02

The changes in the real and imaginary components as an

impact of exposure to thermal stresses are reflected in the Nyquist plot of the coil impedance at all hours of aging, shown in Fig. 7. By the literature handling the characterisation of electrical machine windings and insulation as described in Sections I & II, the main effect of thermal degradation is the drop of the global capacitance in the winding. This can be due to several factors, some of which being expansion of the insulation layers and conductor coating, gases emitted within epoxies and polymers by the thermal stresses that result in air voids imposing porosity within the insulating material, as well as diminishing of the insulating materials' dielectric properties due to decrease of the dielectric strength. With the use of impedance spectroscopy, the latter mechanism and the phenomena involved in the relaxation and transition processes of the real and complex part of the dielectric permittivity are reflected in the real and imaginary part of the total complex coil impedance.

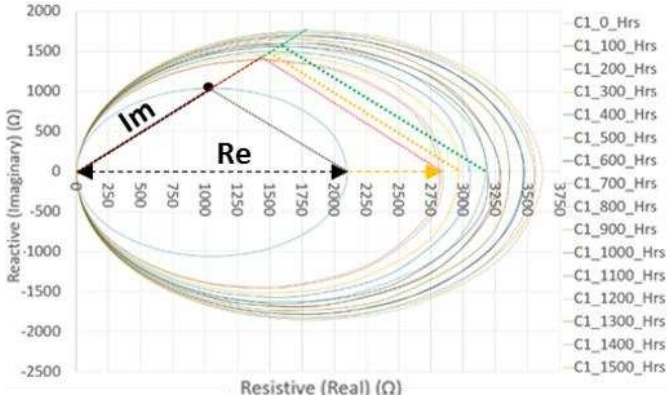


Fig. 7. Evolution of the Real and Imaginary components in the impedance Nyquist locus for coil C1 with respect to the hours of thermal ageing.

This drop in the global capacitance will lead to an increase of the real component ($Re\{Z\}$) as well as of the imaginary component ($Im\{Z\}$). For the coils examined in this study, the network of the circuit model is shown in Fig. 8 accounting for the turn-to-turn capacitance and resistance for one coil side. For the simplified equivalent representation of this network into a circuit of R , L , and C elements as shown in Fig. 9, the impact of the discussed capacitive phenomena demonstrated by the Nyquist plots shows the same effect of under decreasing capacitance in the network. With respect to the frequency sweep performed by impedance spectroscopy, the function of the global impedance $Z(\omega)$ over the frequency spectrum is:

$$Z(\omega) = |Z| \angle \varphi = Re\{Z\} + j \cdot Im\{Z\}, \quad (1)$$

where $|Z|$ is the impedance amplitude, φ the phase angle, while $Re\{Z\}$ and $Im\{Z\}$ express the real and imaginary part of the total complex impedance, respectively:

$$Re\{Z\} = \omega / [(1 - \omega^2 CL)^2 + (\omega RC)^2], \quad (2)$$

$$Im\{Z\} = \omega(L - R^2C - \omega^2 CL^2) / [(1 - \omega^2 CL)^2 + (\omega RC)^2]. \quad (3)$$

In (2) and (3), R is the total coil resistance, L the total

inductance, and C the global capacitance representing the capacitive elements of the coil. Additionally, the natural undamped resonance frequency f_o of the system, with $f_o = 1/[(2\pi)(LC)^{1/2}]$, defines the electrical resonance or maximum frequency f_{max} where the impedance amplitude becomes maximum as in Fig. 5 with f_{max} being:

$$f_{max} = f_o [(1 - 1/(2QL)^4)^{1/2}], \quad (4)$$

where $Q_L = 2\pi f_o L/R$ is the quality factor. As discussed by [51], thermal degradation has a direct impact on the amplitude term of (1), while the angle term remains unaffected [14]. The terms of (2) and (3) are examined via their loci in the Nyquist plots, as illustrated through the measurement results presented in Fig. 7 and the model results in Fig. 9. The resonance frequency given by (4) shifts towards higher ends of the spectrum with the progression of thermal aging, in tandem with an increase in the amplitude term of (1) as illustrated through Fig. 5. With the progression of thermal degradation, there is a diminishing effect of the dielectric strength in the insulating materials. This drop in dielectric permittivity is accommodating a drop in the capacitances of the system, which leads to a drop in the total capacitance. This is directly reflected in the terms given through (1)-(4), as evident by Fig. 5, as well as in the impedance Nyquist plot where the locus is continuously expanding due to the increase of the amplitude term. An additional validation of this rationale is provided through Fig. 9 for the generic case of a coil being represented by a simplified equivalent, where the locus of the impedance real and imaginary components is expanding with respect to decreasing capacitance in agreement with the experimental measurements illustrated in Fig. 5.

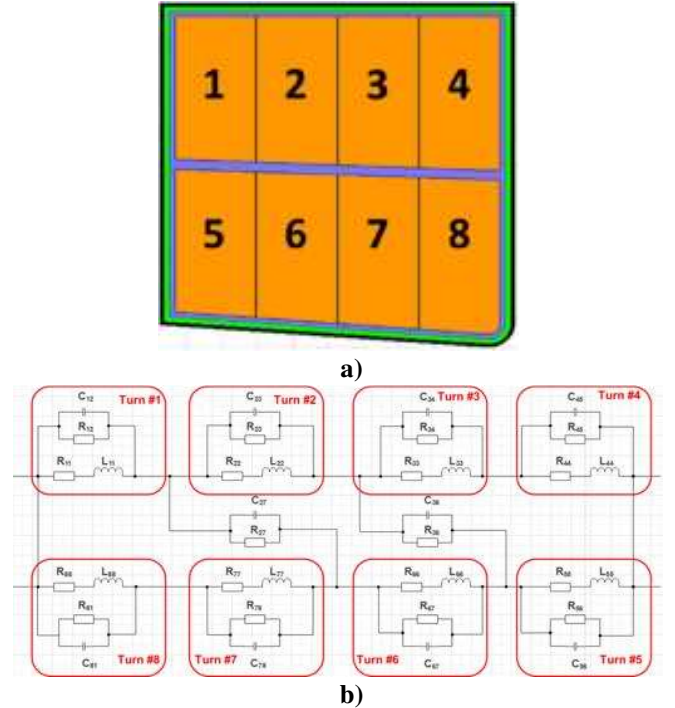


Fig. 8. a) Cross-section of the coil side and bundle of turns, and b) Network of the equivalent circuit model with the turn-to-turn resistances & capacitances for one coil side.

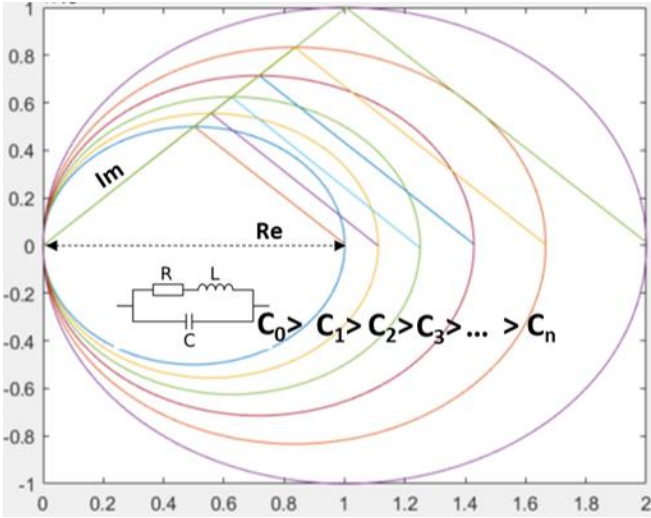


Fig. 9. Evolution of the Real and Imaginary components in the impedance Nyquist plot of a coil simplified R, L, C equivalent with respect to the decrease in the total equivalent capacitance.

B. Validation of Spectroscopy Results by Simulations

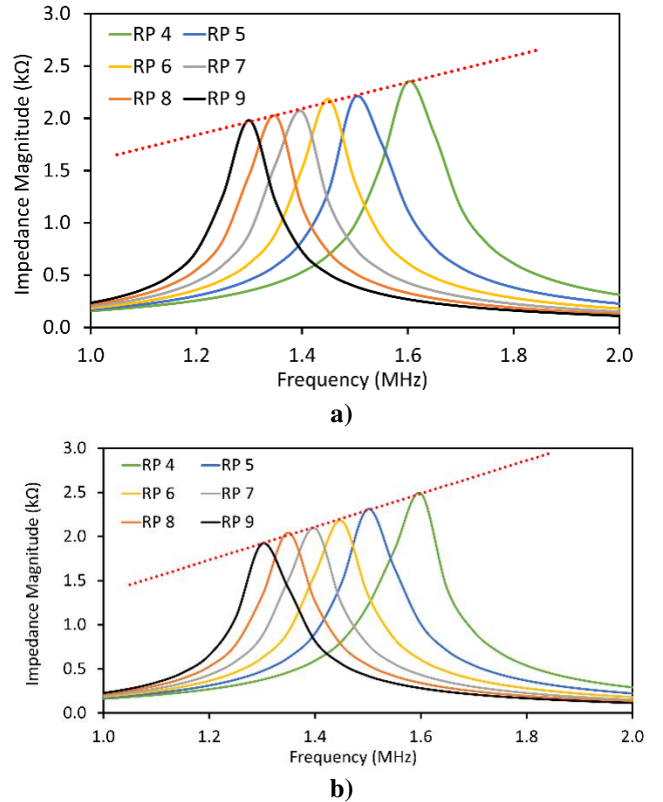
A 2-dimensional (2D) FEA model was created representing the coil geometry, material layers and characteristics, to perform several electrostatic simulations at several different frequency points using the ANSYS software package, emulating the experimental frequency sweeps. The model was exploited in tandem with an electrical circuit equivalent to facilitate a co-simulation setting, where the outputs of the 2D FEA simulations were imported into the MATLAB and LT-Spice software packages to acquire each individual parameter of the electrical equivalent and calculate the impedance inductive and capacitive terms for extraction of the global impedance of the 2D coil representation in the model [52].

In the initial simulation set, a pre-defined value of dielectric permittivity was assigned per insulation layer according to the materials used in the coil (Table I). Then, a series of simulations were run at several frequency points to acquire the baseline healthy coil model response. Several additional simulation sets were created, where diminishing insulation effects were implemented in the permittivity of the insulating materials for each set by dropping the material relative permittivity (RP) by 10% in every simulation set. The process was repeated for the several frequency points as described in the initial simulation step. The collection of impedance data at these different frequency points allowed the acquisition of the frequency responses over the spectrum, corresponding to the frequency sweep experimentally performed with impedance spectroscopy.

The simulation results are presented in Fig. 10. Fig. 10a illustrates the impedance response of the coil model when 10% drops are implemented in the permittivity of the groundwall insulation and overcoat layers, while the rest of the insulation layers are kept intact. The reason for demonstrating this case is that the external layers are the ones affected first by the thermal exposure, so any initial effects in the equivalent circuit terms will be observed through changes in these elements. The result is very similar in Fig. 10b, demonstrating the frequency response when 10% gradual drops take place in the turn

insulation elements only. To consider a holistic effect of the coil insulation system's strength having diminished as during degradation, in Fig. 10c the frequency response is presented for the case where all insulating material layers in the coil have a gradual reduction of relative permittivity by 10% in each simulation set. The simulation results of all cases considered agree with the measurements demonstrated through Section III.

Additionally, Fig. 11 depicts the evolution of the Nyquist plot of the real and imaginary parts of the coil total impedance from the extensive 2D FEA model simulations for gradual drops in the relative permittivity of all the elements in the coil insulation system. Starting from the baseline model depicted with blue colour in Fig. 11, the impedance locus is expanding with the consecutive drops in the relative permittivity. This reflects the gradual drops in the electrical equivalent capacitive terms of the coil insulating system, validating the rationale outlined through Section III for the acquisition of the Nyquist locus evolution acquired in the experimental measurements to map the degradation profile of the examined coils. As evident by Fig. 11, there is a slight difference in the shape of the Nyquist trajectory noticeable in the healthy baseline model with respect to the response observed in the experimental measurements of Fig. 7 and the simplified coil equivalent response of Fig. 9. This difference is attributed to the frequency resolution imposed by the simulation steps and the discretised frequency points selected to emulate the frequency sweep for each simulation set. Additionally, although the electric equivalent circuit considered accounts for turn-to-turn and end-effects increasing the fidelity of the modelling approach, the FEA representation of the coil in the simulation environment is a 2D geometry which deviates from the actual 3D physical structure of the coil assembly.



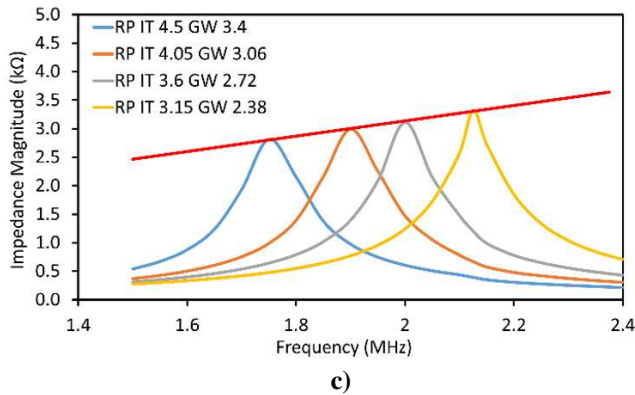


Fig. 10. Impedance frequency response of the 2D FEA model with incremental 10% drops in relative permittivity: a) in the groundwall and overcoat insulation layers, b) in the turn insulation, and c) in all components of the insulating system.

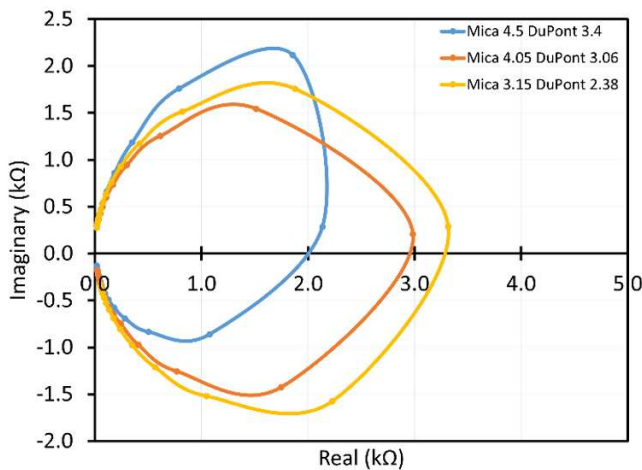


Fig. 11. Impedance Nyquist locus of the 2D FEA model with incremental 10% drops in all insulating components.

V. CONCLUSION & FUTURE WORK

This paper presented a novel approach for mapping the thermal degradation profile of insulation in concentrated stator coils using the impedance frequency response via the Bode and Nyquist plots. The impact of thermal degradation was examined on the insulation system of the coil assemblies from the concentrated stator winding of a PMSG used in the propulsion system of a hybrid aircraft. Ex-situ inspection of the generator coils by means of impedance spectroscopy facilitated the experimental study of the thermal degradation effects on the coil insulation system. Initially, the impact of temperature on the characteristic impedance resonances of the coil were examined with experimental measurements using the impedance Bode plots to conclude on a thermal aging profile by a trendline with respect to the hours of thermal stress. Further, using the impedance Nyquist plots, the response and behavior of the equivalent coil impedance was investigated under thermal aging effects. The thermal degradation mechanism remains persistent with an increasing trend. The extracted thermal degradation profiles and the presented analysis demonstrate the advantage of impedance spectroscopy

as a non-destructive inspection strategy for periodical health assessment. After mapping the degradation profiles experimentally, the paper presented an additional study with FEA simulations investigating the effect of changes in the coil material properties and the impact in the coil electrical equivalent analysis in a co-simulation setting. The simulation results validate the profiles extracted with the experimental measurements, demonstrating the added value of the presented approach and the rationale for using it to map the impedance degradation profile via the frequency responses in combination with the Nyquist plots. Despite the accurate model validation, some key differences were observed between the experimental and model simulation data for the coil response at the start-of-life instance. This is due to the resolution imposed by the discretised frequencies in the simulation setting to acquire the individual frequency points during the impedance sweeps, and due to the 2D representation of the coil geometry in the theoretical model versus the 3D physical coil structure.

Aspects of future work include the extraction of the degradation profile up to the point of complete coil failure and quantification of the degradation rates per cycle by metrics to identify indicators for the estimation of the remaining useful life of the coil and its insulation system. Also, the observations and analysis of the impedance components locus via the Nyquist plots enables the potential for failure identification by the pattern of the locus, as well as the setting of thresholds for life limiting factors aiming to the identification and prevention of failure in electrical machine components such as stator winding coils. Further, application of the presented approach for mapping the degradation profile beyond concentrated stator coils aims to be explored, for the generalization of the technique in other types of insulation systems and other types of windings such as distributed windings.

ACKNOWLEDGMENT

The authors would like to acknowledge Viljar Fjellanger from Rolls-Royce Plc Electrical, Norway, for the provision of test hardware and FAT data to The University of Sheffield, UK.

REFERENCES

- [1] Stone, G. C., Boulter, E. A., Culbert, I., & Dhirani, H. (2004). *Electrical insulation for rotating machines: design, evaluation, aging, testing, and repair* (Vol. 21). John Wiley & Sons.
- [2] Hemmati, R., Wu, F., & El-Refai, A. (2019, May). Survey of insulation systems in electrical machines. In *2019 IEEE International Electric Machines & Drives Conference (IEMDC)* (pp. 2069-2076). IEEE.
- [3] Höpner, V. N., & Wilhelm, V. E. (2021). Insulation Life Span of Low-Voltage Electric Motors—A Survey. *Energies*, 14(6), 1738.
- [4] Madonna, V., Giangrande, P., & Galea, M. (2018). Electrical power generation in aircraft: Review, challenges, and opportunities. *IEEE Transactions on Transportation Electrification*, 4(3), 646-659.
- [5] Borghei, M., & Ghassemi, M. (2021). Insulation materials and systems for more-and all-electric aircraft: A review identifying challenges and future research needs. *IEEE Transactions on Transportation Electrification*, 7(3), 1930-1953.
- [6] Panagiotou, P. A., Lambourne, A., & Jewell, G. W. (2022, September). Survey of Insulation in Electrical Machines for Aerospace: Systems, Materials & Inspection. In *2022 International Conference on Electrical Machines (ICEM)* (pp. 2318-2324). IEEE.
- [7] Sarlioglu, B., & Morris, C. T. (2015). More electric aircraft: Review, challenges, and opportunities for commercial transport aircraft. *IEEE transactions on Transportation Electrification*, 1(1), 54-64.

- [8] Perisse, F., Werynski, P., & Roger, D. (2007). A new method for AC machine turn insulation diagnostic based on high frequency resonances. *IEEE Transactions on Dielectrics and Electrical Insulation*, 14(5), 1308-1315.
- [9] Kavanagh, D. F., Howey, D. A., & McCulloch, M. D. (2013, August). An applied laboratory characterisation approach for electric machine insulation. In 2013 9th IEEE International Symposium on Diagnostics for Electric Machines, Power Electronics and Drives (SDEMPED) (pp. 391-395). IEEE.
- [10] Neti, P., & Grubic, S. (2016). Online broadband insulation spectroscopy of induction machines using signal injection. *IEEE Transactions on Industry Applications*, 53(2), 1054-1062.
- [11] Tripathi, A. N., Iqbal, A., & Das, S. (2019, November). Understanding the Aging of XLPE Cable Insulation Using Impedance Analyzer. In 2019 International Conference on Electrical, Electronics and Computer Engineering (UPCON) (pp. 1-5). IEEE.
- [12] Moreno, Y., Egea, A., Almandoz, G., Ugalde, G., Urdangarin, A., & Moreno, R. (2022, September). High-Frequency Modelling of Windings. In 2022 International Conference on Electrical Machines (ICEM) (pp. 1232-1238). IEEE.
- [13] Ruiz-Sarrio, J. E., Chauvicourt, F., & Martis, C. (2022, September). Sensitivity Analysis of a Numerical High-Frequency Impedance Model for Rotating Electrical Machines. In 2022 International Conference on Electrical Machines (ICEM) (pp. 1260-1266). IEEE.
- [14] Panagiotou, P. A., Lambourne, A., & Jewell, G. W. (2022, September). Ex-situ Inspection of Concentrated Stator Coils by Means of Impedance Spectroscopy. In 2022 International Conference on Electrical Machines (ICEM) (pp. 2331-2337). IEEE.
- [15] Rao, B. N., Sudhindra, A., & Ramachandra, B. (2009, July). Low frequency dielectric response of thermally degraded epoxy-mica insulation. In 2009 IEEE 9th International Conference on the Properties and Applications of Dielectric Materials (pp. 1026-1029). IEEE.
- [16] Fernando, M. A. R. M., Naranpanawa, W. M. L. B., Rathnayake, R. M. H. M., & Jayantha, G. A. (2013). Condition assessment of stator insulation during drying, wetting and electrical ageing. *IEEE Transactions on Dielectrics and Electrical Insulation*, 20(6), 2081-2090.
- [17] Homagk, C., Mossner, K., & Leibfried, T. (2008, October). Investigation on degradation of power transformer solid insulation material. In 2008 Annual Report Conference on Electrical Insulation and Dielectric Phenomena (pp. 75-78). IEEE.
- [18] M. Sumislawska, K. N. Gyftakis, D. F. Kavanagh, M. D. McCulloch, K. J. Burnham, and D. A. Howey, "The Impact of Thermal Degradation on Properties of Electrical Machine Winding Insulation Material", *IEEE Trans. Ind. Appl.*, Vol. 52, No. 4, pp. 2951-2960, Jul/Aug 2016.
- [19] Farahani, M., Gockenbach, E., Borsi, H., Schäfer, K., & Kaufhold, M. (2010). Behavior of machine insulation systems subjected to accelerated thermal aging test. *IEEE Transactions on Dielectrics and Electrical Insulation*, 17(5), 1364-1372.
- [20] Wang, H., & Busch, R. (1998, June). A discussion of some concepts in thermal aging test-thermal aging and thermal breakdown. In ICSD'98. Proceedings of the 1998 IEEE 6th International Conference on Conduction and Breakdown in Solid Dielectrics (Cat. No. 98CH36132) (pp. 443-446). IEEE.
- [21] Sumereder, C., Muhr, M., Marketz, M., Rupp, C., & Kruger, M. (2009). Unconventional diagnostic methods for testing generator stator windings. *IEEE Electrical Insulation Magazine*, 25(5), 18-24.
- [22] Hoang, A. T., Serdyuk, Y. V., & Gubanski, S. M. (2014). Electrical characterization of a new enamel insulation. *IEEE Transactions on Dielectrics and Electrical Insulation*, 21(3), 1291-1301.
- [23] Hassan, O., Shyegani, A. A., Borsi, H., Gockenbach, E., Abu-Elzahab, E. M., & Gilany, M. I. (2004, July). Detection of oil-pressboard insulation aging with dielectric spectroscopy in time and frequency domain measurements. In Proceedings of the 2004 IEEE International Conference on Solid Dielectrics, 2004. ICSD 2004. (Vol. 2, pp. 665-668). IEEE.
- [24] Lee, S. B., Tallam, R. M., & Habetler, T. G. (2003). A robust, on-line turn-fault detection technique for induction machines based on monitoring the sequence component impedance matrix. *IEEE Transactions on Power Electronics*, 18(3), 865-872.
- [25] Deloglu, G., Porru, M., & Serpi, A. (2021, October). A Brief Overview on Commercial Aircraft Electrification: Limits and Future Trends. In 2021 IEEE Vehicle Power and Propulsion Conference (VPPC) (pp. 1-5). IEEE.
- [26] Da Silva, F. F., Fernandes, J. F., & da Costa Branco, P. J. (2021). Barriers and challenges going from conventional to cryogenic superconducting propulsion for hybrid and all-electric aircrafts. *Energies*, 14(21), 6861.
- [27] Ghassemi, M., Barzkar, A., & Saghafi, M. (2022). All-Electric NASA N3-X aircraft electric power systems. *IEEE Transactions on Transportation Electrification*, 8(4), 4091-4104.
- [28] Fard, M. T., & He, J. (2021, October). Comparison of medium-voltage high-frequency power inverters for aircraft propulsion drives. In 2021 IEEE Energy Conversion Congress and Exposition (ECCE) (pp. 1599-1605). IEEE.
- [29] Trentin, A., Sala, G., Tarisciotti, L., Galassini, A., Degano, M., Connor, P. H., ... & Gerada, C. (2020). Research and realization of high-power medium-voltage active rectifier concepts for future hybrid-electric aircraft generation. *IEEE Transactions on Industrial Electronics*, 68(12), 11684-11695.
- [30] Jiang, J., Wang, K., Chen, L., Cotton, I., Chen, J., Chen, J., & Zhang, C. (2020). Optical sensing of partial discharge in more electric aircraft. *IEEE Sensors Journal*, 20(21), 12723-12731.
- [31] Bartnikas, R., & Morin, R. (2004). Multi-stress aging of stator bars with electrical, thermal, and mechanical stresses as simultaneous acceleration factors. *IEEE transactions on energy conversion*, 19(4), 702-714.
- [32] Verginadis, D., Falekas, G., Mavrommatis, V., Karlis, A., Danikas, M. G., & Antonino-Daviu, J. A. (2022, September). Investigation of How Partial Discharges Affect Mica and Epoxy Resin: Simulations and Reference on Electrical Machines' Insulation. In 2022 International Conference on Electrical Machines (ICEM) (pp. 2351-2357). IEEE.
- [33] Ji, Y., Giangrande, P., Madonna, V., Zhao, W., Galea, M., Li, J., & Zhang, H. (2022, September). Investigation on Humidity Effect on Partial Discharge Considering Thermal Aging. In 2022 International Conference on Electrical Machines (ICEM) (pp. 2325-2330). IEEE.
- [34] Sundeep, S., Wang, J., Griffo, A., & Alvarez-Gonzalez, F. (2021). Antiresonance phenomenon and peak voltage stress within PWM inverter fed stator winding. *IEEE Transactions on Industrial Electronics*, 68(12), 11826-11836.
- [35] Gardner, R., Cotton, I., & Kohler, M. (2015, June). Comparison of power frequency and impulse based Partial Discharge measurements on a variety of aerospace components at 1000 and 116 mbar. In 2015 IEEE Electrical Insulation Conference (EIC) (pp. 430-433). IEEE.
- [36] Haghghi, H., Cotton, I., Gardner, R., & Sauvage, B. (2018). Definitions of Test Conditions for High Voltage Aerospace Systems Using the IAGOS Atmospheric Dataset (No. 2018-01-1931). SAE Technical Paper.
- [37] Torkaman, H., & Karimi, F. (2015). Influence of ambient and test conditions on insulation resistance/polarization index in HV electrical machines-a survey. *IEEE Transactions on Dielectrics and Electrical Insulation*, 22(1), 241-250.
- [38] Farahani, M., Borsi, H., & Gockenbach, E. (2007). Study of capacitance and dissipation factor tip-up to evaluate the condition of insulating systems for high voltage rotating machines. *Electrical Engineering*, 89, 263-270.
- [39] Huang, Z., Reinap, A., & Alaküla, M. (2016, September). Dielectric properties modeling and measurement of single tooth coil insulation system under accelerated degradation test. In 2016 XXII International Conference on Electrical Machines (ICEM) (pp. 2698-2703). IEEE.
- [40] Farahani, M., Borsi, H., & Gockenbach, E. (2004, July). Dielectric spectroscopy in time and frequency domain on insulation system of high voltage rotating machines. In Proceedings of the 2004 IEEE International Conference on Solid Dielectrics, 2004. ICSD 2004. (Vol. 1, pp. 60-63). IEEE.
- [41] Rieux, N., Pouilles, V., & Lebey, T. (1994, October). Dielectric spectroscopy of epoxy based insulation systems aged under functional electrical and thermal conditions. In Proceedings of IEEE Conference on Electrical Insulation and Dielectric Phenomena-(CEIDP'94) (pp. 361-366). IEEE.
- [42] David, É., & Lamarre, L. (2005). Influence of rise time on dielectric parameters extracted from time domain spectroscopy in the context of generator stator insulation. *IEEE transactions on dielectrics and electrical insulation*, 12(3), 423-428.
- [43] Wang, H., & Busch, R. (1998, June). A discussion of some concepts in thermal aging test-thermal aging and thermal breakdown. In ICSD'98. Proceedings of the 1998 IEEE 6th International Conference on Conduction and Breakdown in Solid Dielectrics (Cat. No. 98CH36132) (pp. 443-446). IEEE.
- [44] Kremer, F., & Schönhals, A. (Eds.). (2002). *Broadband dielectric spectroscopy*. Springer Science & Business Media.

- [45] Hirai, N., Yamada, T., & Ohki, Y. (2012, September). Comparison of broadband impedance spectroscopy and time domain reflectometry for locating cable degradation. In 2012 IEEE International Conference on Condition Monitoring and Diagnosis (pp. 229-232). IEEE.
- [46] Morin, R., Novak, J. P., Bartnikas, R., & Ross, R. (1995). Analysis of in-service aged stator bars. *IEEE transactions on energy conversion*, 10(4), 645-654.
- [47] Philippe, L. V. S., Walter, G. W., & Lyon, S. B. (2003). Investigating localized degradation of organic coatings: comparison of electrochemical impedance spectroscopy with Local Electrochemical Impedance Spectroscopy. *Journal of the electrochemical society*, 150(4), B111.
- [48] Zhou, Z., Zhang, D., He, J., & Li, M. (2015). Local degradation diagnosis for cable insulation based on broadband impedance spectroscopy. *IEEE Transactions on Dielectrics and Electrical Insulation*, 22(4), 2097-2107.
- [49] Macdonald, J. R., & Barsoukov, E. (Eds.). (2018). *Impedance spectroscopy: theory, experiment, and applications*. John Wiley & Sons.
- [50] E. J. W. Stone, P. A. Panagiotou, J. Mühlthaler, A. R. Mills, A. Lambourne and G. W. Jewell, "Identification of Thermal Failure Profiles in Stator Winding Insulation by Impedance Spectroscopy," 2024 International Conference on Electrical Machines (ICEM), Torino, Italy, 2024, pp. 1-7, doi: 10.1109/ICEM60801.2024.10700564.
- [51] P. A. Panagiotou, E. J. W. Stone, J. Mühlthaler, A. Reeh, A. Lambourne and G. W. Jewell, "Thermal Degradation Profile of Concentrated Stator Winding Insulation by Impedance Spectroscopy", 2023 IEEE 14th International Symposium on Diagnostics for Electrical Machines, Power Electronics and Drives (SDEMPED), Chania, Greece, 2023, pp. 554-560.
- [52] E. J. W. Stone, P. A. Panagiotou, J. Mühlthaler, A. R. Mills, A. Lambourne and G. W. Jewell, "Modelling of Insulation in Concentrated Stator Coils for Characterisation and Material Changes," 2024 International Conference on Electrical Machines (ICEM), Torino, Italy, 2024, pp. 01-08, doi: 10.1109/ICEM60801.2024.10700317.



Edward J. W. Stone received the B.Eng. degree in electrical engineering from Sheffield Hallam University, Sheffield, U.K., in 2016, and the Ph.D. degree in synchronous reluctance machines from the Department of Electronic and Electrical Engineering of the University of Sheffield, Sheffield, U.K., in 2021.

Since receiving his Ph.D. degree in 2021, he is a Postdoctoral Research Associate with the Electrical Machines and Drives research group of the School of Electrical and Electronic Engineering of the University of Sheffield, Sheffield, U.K., working at the Rolls-Royce University Technology Centre in Advanced Electrical Machines of the University of Sheffield. His research interests include electrical machine design, Class D amplification, insulation monitoring and degradation, as well as inspection and repair technologies for electrical machines.

Dr. Stone is a member of the Institution of Engineering and Technology (IET, U.K.).



Panagiotis A. Panagiotou (M'22) received the 5-year Diploma (B.S. & M.Eng.) from the Department of Electrical and Computer Engineering of the University of Patras, Patras, Greece, in 2015, and the M.Sc. degree in Complex Systems and Network Theory from the Department of

Mathematics of the Aristotle University of Thessaloniki, Thessaloniki, Greece, in 2017. He received the Ph.D. degree in fault diagnostics of electrical machines from Coventry University, Coventry, U.K., in 2020.

In 2021, he joined the Department of Electronic and Electrical Engineering of the University of Sheffield, Sheffield, U.K., as a postdoctoral research associate at the Rolls-Royce University Technology Centre for Advanced Electrical Machines of the University of Sheffield. Since 2022, he is a Lecturer in electrical machines with the School of Electrical and Electronic Engineering of the University of Sheffield, Sheffield, U.K. His research interests include condition monitoring, fault detection and diagnostics in electrical machines, signal processing for diagnostics, and technologies for the inspection and repair of electrical machines.

Dr. Panagiotou is a member of the IEEE, a member of the Institution of Engineering and Technology (IET, U.K.) and a Fellow of the Higher Education Academy (FHEA), U.K.



Johannes Mühlthaler (Student Member, IEEE, 2024) received the B.Eng. degree in electrical engineering from the University of Applied Sciences, Rosenheim, Germany, in 2017, and the M.Sc. degree in electrical engineering from the Technical University of Munich, Munich, Germany, in 2020.

In 2019, he joined Rolls-Royce Electrical Ltd & Co KG in Munich, Germany where he is currently a doctoral candidate working toward the Ph.D. degree with Rolls-Royce Electrical Ltd. & Co.

Deutschland in Munich, Germany. His current research focuses on the modelling and verification of winding fault effects, fault detection and mitigation strategies in multi-lane permanent magnet synchronous machines.



Andreas Reeh received the Diploma in Mechanical Engineering and the doctorate degree from the Technical University Darmstadt, Darmstadt, Germany, in 2009 and 2014, respectively.

He joined Siemens eAircraft in 2015 researching and developing electrical propulsion systems and in 2019 transitioned to Rolls-Royce Ltd. & Co, Munich, Germany. Since 2016, he has been heading the electrical machine design teams, and since 2022 he is the global competence lead for electromagnetics and thermal design in Rolls-Royce Electrical Ltd. & Co. Deutschland in Munich, Germany. His research interests include advance machine topologies, multi-disciplinary design optimization, fault tolerance and aircraft system interactions.



Alexis Lambourne received the B.Eng. degree in materials engineering from Loughborough University, U.K., in 1999 and the Ph.D. degree from Oxford University, Oxford, U.K., in 2003. He joined Rolls-Royce Submarines in 2003, and since 2005 he has been working for Rolls-Royce Plc. Central Technologies as a materials specialist in novel and emerging materials technologies.

From 2014-2017, he held a Royal Society industrial fellowship on the materials challenges for hybrid aerospace. His research focuses on the materials and manufacturing of high-power density electrical systems in aerospace environments, including materials selection, testing, degradation, inspection, and recycling. His research interests include a wide variety of functional, smart, and nano materials as well as their applications in aerospace and electric power systems.



Geraint W. Jewell received the B.Eng. and Ph.D. degrees in electrical engineering from the University of Sheffield, Sheffield, U.K., in 1988 and 1992, respectively. Since 1994, he has been a member of the academic staff with

the School of Electrical and Electronic Engineering of the University of Sheffield, where he is a professor of electrical engineering.

He held an Engineering and Physical Sciences Research Council (EPSRC) Advanced Research Fellowship from 2000 to 2005 and a Royal Society Industry Fellowship with Rolls-Royce from 2006 to 2008. He is currently the director at the Rolls-Royce University Centre in Advanced Electrical Machines of the University of Sheffield, and the director at the EPSRC Future Electrical Machines Manufacturing Hub. His research interests include the modelling and design of a wide variety of electromagnetic devices, notably electrical machines

for aerospace, electro-mechanical actuators, and high-temperature applications.